Variable aging and storage of dissolved black carbon in the ocean

Journal Article

Author(s):
Coppola, Alysha I.; Druffel, Ellen R.M.; Broek, Taylor A.; Haghipour, Negar; Eglinton, Timothy I.; McCarthy, Matthew; Walker, Brett D.

Variable aging and storage of dissolved black carbon in the ocean

Alysha I. Coppola[a], Ellen R. M. Druffel[b,1], Taylor A. Broek[c], Negar Haghipour[a,d], Timothy I. Eglinton[a], Matthew McCarthy[e], and Brett D. Walker[b,f]

During wildfires and fossil fuel combustion, biomass is converted to black carbon (BC) via incomplete combustion. BC enters the ocean by rivers and atmospheric deposition contributing to the marine dissolved organic carbon (DOC) pool. The fate of BC is considered to reside in the marine DOC pool, where the oldest BC ^{14}C ages have been measured (>20,000 ^{14}C y), implying long-term storage. DOC is the largest exchangeable pool of organic carbon in the oceans, yet most DOC (>80%) remains molecularly uncharacterized. Here, we report ^{14}C measurements on size-fractionated dissolved BC (DBC) obtained using benzene polycarboxylic acids as molecular tracers to constrain the sources and cycling of DBC and its contributions to refractory DOC (RDOC) in a site in the North Pacific Ocean. Our results reveal that the cycling of DBC is more dynamic and heterogeneous than previously believed though it does not comprise a single, uniformly "old" ^{14}C age. Instead, both semilabile and refractory DBC components are distributed among size fractions of DOC. We report that DBC cycles within DOC as a component of RDOC, exhibiting turnover in the ocean on millennia timescales. DBC within the low-molecular-weight DOC pool is large, environmentally persistent and constitutes the size fraction that is responsible for long-term DBC storage. We speculate that sea surface processes, including bacterial remineralization (via the coupling of photooxidation of surface DBC and bacterial co-metabolism), sorption onto sinking particles and surface photochemical oxidation, modify DBC composition and turnover, ultimately controlling the fate of DBC and RDOC in the ocean.

dissolved organic carbon | dissolved black carbon | ocean carbon cycle | refractory and semilabile DOC | size-fractionated DOC

Wildfires and fossil fuel combustion produce large amounts of greenhouse gases and charred residues, including black carbon (BC). BC is operationally defined as the carbonaceous, polycondensed aromatic products (>60% organic carbon) derived from the incomplete combustion of biomass and fossil fuels (1, 2). It represents a continuum of polycyclic aromatic structures with high molecular diversity, thus imparting resistance to chemical and biological degradation in soils (3, 4) and persisting on timescales of centuries to millennia in the environment (1). The majority of BC is produced by wildfires (128 ± 84 to 153 ± 18 Tg BC y^{-1}), of which most is left behind on the landscape, while a small fraction (2 to 11 Tg BC per year) is emitted to the atmosphere as soot (5, 6). BC production from wildfires is several orders of magnitude greater than that from fossil fuel burning (2 to 29 Tg y^{-1}) (7, 8).

BC produced by fires represents a significant long-term sink of CO_2, due to its environmentally persistent properties when compared to the original biomass. Because wildfires change labile biomass carbon to more environmentally refractory and slowly cycling BC (6,000 to 23,000 ^{14}C y) (9, 10), they influence rates of turnover in the global carbon cycle. Production of BC is particularly relevant in the context of carbon sequestration in a warming climate given projected increases in fire severity, extent, and amplitude (11, 12). BC is considered the oldest and most abundant molecularly characterized component of the modern carbon cycle (9, 10), with long-term apparent persistence in the environment (1, 5). Omitting BC production from assessments of fire impacts on the carbon cycle leads to overestimation of the strength of positive feedbacks between climate change and wildfire emissions (5, 13–15). Modeling studies suggest that BC cycling may likely reduce the future increase in atmospheric CO_2 (4 to 8 Pg from 2000 to 2300) with an increasing future wildfire regime (in Representative Concentration Pathways to 4.5 and 8.5) (13). However, significant uncertainties exist with respect to BC budgets, including fluxes between and turnover within different carbon reservoirs. As an example, the large inconsistencies currently exist between estimates of the turnover of dissolved BC (DBC) in the ocean based on apparent ^{14}C ages determined via geochemical methods and BC turnover rates inferred by mass balance equations (1). Currently, isotopic measurements

Significance

During wildfires, substantial amounts of biomass are converted to charred by-products, rich in black carbon (BC), produced via incomplete combustion. BC enters the ocean by rivers and atmospheric deposition and contributes to the marine dissolved organic carbon (DOC) pool. Dissolved BC (DBC) in seawater is a minor component of the marine DOC but is a significant component of the refractory DOC pool.

Author affiliations: [a]Department of Earth Sciences, Geological Institute, ETH Zürich, Zürich 8092, Switzerland; [b]Department of Earth System Science, University of California, Irvine, CA 92697; [c]Geology and Geophysics Department, Woods Hole Oceanographic Institution, Woods Hole, MA 02543; [d]Laboratory of Ion Beam Physics, ETH Zürich, Zürich 8093, Switzerland; [e]Department of Ocean Science, University of California, Santa Cruz, CA 95064; and [f]Department of Earth and Environmental Sciences, University of Ottawa, Ottawa, ON K1N 6N5, Canada

of DBC in the deep ocean remain too few (n = 8) (9, 10, 16) to constrain the age, cycling and fate of marine BC and assess the importance of BC as a negative feedback in the global carbon cycle.

BC is produced on land, mobilized from soils by erosion, and delivered to the oceans by fluvial and atmospheric transport. After a wildfire, the majority of BC remains on the landscape as charcoal, and a small fraction is emitted and airborne as soot BC (8, 17). The biomass burning aerosol soot BC Δ^{14}C endmembers are generally modern (>0‰) but can contain a background mixture of soot BC from fossil fuels during low fire activity (–354 ± 6‰) (18). The flux of soot BC deposited by aerosols to the surface ocean has been estimated at 1.8 Tg C y^{-1} (7) with Δ^{14}C values ranging from –1000‰ to –600‰ (19). After a wildfire, only <14% of BC remains in soils (20). BC on land is transferred into aquatic systems via erosion and weathering processes (via chemical and photo-oxidation and biotic degradation) (21, 22) that produce particulate and water-soluble DBC components, which can ultimately be transported to the coastal and open ocean (23). River DOC (dissolved organic carbon) contains about 12 ± 5% (DBC/DOC%) of DBC (at a global flux of 18 ± 4 Tg y^{-1}) (24–26), irrespective of fire frequency (25, 27, 28). Charcoal is eroded from the hillslope following a fire, as the primary driver of Particulate BC (PBC) export (28, 29). We focus on marine DBC because there is a discrepancy between the modern age and flux of DBC exported by rivers and the pool size and radiocarbon (^{14}C) age of marine DBC (14 to 36 Pg, –945 ± 6‰, 23,000 ± 3,000 ^{14}C y) (9, 30). Also, the stable carbon isotopic composition (δ^{13}C values) of DBC in river and marine waters reveals a significant discrepancy, suggesting large DBC losses at the river–ocean interfaces and/or a nonterrestrial source (31). This discrepancy, combined with poor constraints on stocks and sinks, highlights the poor current constraints on DBC sources and cycling (1).

Upon entering the oceans, DBC becomes a component of the marine carbon cycle (32). Marine DOC (passing through a 0.2 to 1 μm filter) represents the largest reservoir of organic matter in the ocean (662 Pg C) (33) and constitutes among the most complex mixture of compounds on Earth (33, 34). DOC also comprises a continuum of molecular sizes that exhibit a range of ^{14}C ages (35). Most DOC released by phytoplankton is consumed by heterotrophic microbes within hours to days. For currently unknown reasons, a residual fraction of DOC resists biological decomposition and enters the refractory DOC (RDOC) pool, where it can persist in the ocean for millennia (10, 36). The total DOC pool is roughly 3,000 ^{14}C y older than expected from the global transport time associated deep ocean thermohaline circulation (37, 38). Within the DOC pool, a clear relationship exists between molecular size and reactivity such that the high-molecular-weight (HMW, >1,000 Da) fraction of DOC is composed of predominantly semilabile compounds. In contrast, the low-molecular-weight (LMW, <1,000 Da) DOC is considered to comprise mainly refractory compounds (39, 40). DOC also follows a size–age–composition continuum with younger ^{14}C ages in HMW DOC and older ^{14}C ages in LMW DOC (41). DBC has been inferred to contribute to the RDOC pool given that DBC is the oldest and most abundant reported DOC compound class in the ocean (2 to 6% of marine DOC, 12 to 14 Pg DBC) (9, 42). The average ^{14}C age of DBC in surface waters is 4,800 ± 600 y (n = 6, –450‰ ± 42‰) and 23,100 ± 300 y (n = 2, –918‰ ± 21‰) (10, 43) in the deep ocean, the latter being approximately four times older than bulk DOC, implying that DBC influences bulk DOC ^{14}C age distributions. Thus, marine DBC, despite larger variations in age and likely reactivity, is inert on the timescales of ocean mixing and therefore is a key component of RDOC (44). Prior measurements

of surface and deep ocean DBC concentrations and ^{14}C ages suggest the presence of two components: a modern, fluvially derived DBC pool and a well-mixed background aged DBC pool, much like has been inferred for DOC (9, 26).

The origin of RDOC (630 Pg) has puzzled marine biogeochemists for decades. It is not known how or why RDOC persists for millennia, when the majority of DOC is believed to be produced by marine phytoplankton at the sea surface (45). After production by phytoplankton, most DOC is consumed by marine heterotrophs. One proposed concept is the microbial carbon pump that attributes RDOC formation to successive microbial processing of organic matter, leading to an intrinsic recalcitrant nature of DOC (44, 46, 47). A second concept proposes emergent recalcitrance, where DOC is continuously reworked by marine heterotrophs on all scales, and recalcitrance emerges on an ecosystem level through extreme chemical diversity and dilution of individual compound concentrations (48). A third hypothesis is the input of ^{14}C-free DOC into the marine pool by either hydrothermal vents (49), natural asphalt, methane, and oil seeps (50–52) or refractory DBC, explored here (10, 49).

Here, to further understand the old ^{14}C-age of DOC and the cycling of DBC, we use benzene polycarboxylic acids (BPCAs) as molecular markers of fire-derived BC, determining their abundance and radiocarbon signatures (Δ^{14}C values) in size-fractionated oceanic DOC. These BPCA measurements on HMW and LMW DOC samples taken from the North Pacific Subtropic Gyre are used to assess size–age distributions of DBC in the ocean. This work used a combination of field and lab-based studies. Briefly, seawater was collected using Niskin bottles from the surface mixed layer (7 m) and at depth (2,500 m) at the Hawaii Ocean Time Series (HOT) Station ALOHA (A Long-Term Oligotrophic Habitat Assessment 22°25′N, 158°00′W). We explore DBC characteristics based on the molecular size, using an in-line combination of ultrafiltration (HMW UDOC) and solid-phase extraction (LMW SPE-DOC) (41, 53) to investigate whether DBC also follows size–age relationships akin to DOC (35). We used a wet chemical oxidative hydrolysis method to separate and quantify aromatic moieties as BPCAs that originate from the condensed aromatic structures comprising BC. The number of corresponding BPCAs (B2-B6CAs) from the overall BC structure has different numbers of carboxylic acids present, based on adjacent aromatic groups from which it derived (54). The ratio of different BPCA markers (e.g., B6CA/total BPCAs) can provide information on the degree of aromatic condensation from complimentary studies with ^{13}C NMR spectroscopy (55, 56). Thus, the ratio of BPCA molecular markers (B6CA/total BPCAs) can be used to infer the degree of aromatic condensation (55). The degree of aromatic condensation (56, 57) determines the stability of BC against degradation in the environment (58–60). Specifically, higher degrees of aromatic condensation indicates an overall more polycondensed aromatic structural network (61, 62). DBC characteristics based on size (molecular weight), degree of aromatic condensation, and radiocarbon content provide insights into the composition and turnover of the enigmatic pool of RDOC that is assumed to evade microbial degradation and surface photochemical oxidation for multiple ocean mixing cycles.

1. Results and Discussion

1.1. DBC Concentrations, Distributions, and Isotopic Characteristics. Measured total DOC concentrations at the time of sampling at Station ALOHA in the central Pacific were 75.9 μM and 38.6 μM in the surface (7 m) and deep (2,500 m) ocean, respectively (41) (*SI Appendix*, Table S1A) (Fig. 1). The DOC

concentrations in LMW SPE-DOC are 15.5 µM and 11.7 µM, in the surface and deep samples, respectively. DOC concentrations in HMW UDOC are 12.4 µM in surface waters and 2.5 µM at depth (*SI Appendix,* Table S1A). The Δ^{14}C values for total DOC are –235 ± 2‰ and –552 ± 2‰ in surface and deep waters, respectively. LMW SPE-DOC pools have lower Δ^{14}C values (–343 ± 2‰ and –578 ± 2‰) than those of HMW UDOC (–50 ± 3‰ and –366 ± 2‰) in both the surface and ocean deep, respectively. These data follow a previously reported molecular size–age relationship for DOC where HMW DOC has higher Δ^{14}C values and LMW DOC has lower Δ^{14}C values (35, 53).

Compound-specific measurements of BPCAs reveal that DBC concentrations in LMW SPE-DOC (670 ± 87 nM and 540 ± 88 nM in surface deep waters, respectively) are an order of magnitude higher than those in HMW UDOC (64 ± 23 nM and 32 ± 12 nM, respectively) (Fig. 1B and *SI Appendix,* Table S1B). The proportion of DBC in relation to DOC concentrations (DBC/DOC %) ranged from 0.5 ± 0.3% to 4.6 ± 0.8% (*SI Appendix,* Table S1B), with DBC strongly enriched in the LMW-SPE-DOC fraction of DOC. However, the degree of aromatic condensation is variable in each size class and with depth, ranging from the most polycondensed DBC structure observed in surface HMW UDOC to the least condensed in surface LMW SPE-DOC (65 ± 2% B6CA/sum of BPCAs to 15 ± 2% B6CA/sum BPCAs) (*SI Appendix,* Table S1B). The degree of aromatic condensation is not linked to molecular size, as previous mass spectrometry work found that there was no relationship between number of aromatic rings (molecular weight) and BPCA concentration (62). Thus, the proportion of BPCAs that are liberated from more polycondensed DBC structures provides qualitative distinctions between different types of DBC (62), with more polycondensed structures (given by B6CA and B5CAs) with higher aromaticity compared to less polycondensed structures (B3CA and B4CAs) with more functional groups.

The DBC Δ^{14}C values were measured for two binned groups of BPCA markers, representing more (B6CA+B5CAs) or less polycondensed (B3CA+B4CAs) DBC structures (*Methods*). More polycondensed DBC (B5CA+B6CAs) in LMW SPE-DOC have Δ^{14}C values of –602 ± 230‰ and –417 ± 88‰ in the surface and deep water samples. More polycondensed DBC in HMW UDOC has Δ^{14}C values in surface and deep waters of –272 ± 70‰ and –525 ± 14‰, respectively (*SI Appendix,* Table S1C). Less polycondensed DBC in LMW SPE-DOC has Δ^{14}C values of –582 ± 54‰ and –734 ± 24‰ (*SI Appendix,* Table S1D) and in HMW UDOC has Δ^{14}C values of –822 ± 7‰ and –453 ± 17‰ in the surface and deep samples, respectively (*SI Appendix,* Table S1D). These data indicate that in general, DBC components cycle on longer timescales than those of marine DOC, with the ^{14}C age of DBC size fractions ranging from 2,500 ± 780 to 13,800 ± 300 ^{14}C y in surface and deep waters, respectively, compared to ^{14}C ages of total DOC that are 2,085 ± 25 ^{14}C y, and 6,380 ± 40 ^{14}C y for corresponding surface and deep water samples (41).

1.2. DBC Is Unevenly Distributed among Size Fractions of RDOC.

DOC concentrations decrease by more than half from surface to deep waters, primarily due to biological processes that remove HMW DOC (*SI Appendix,* Table S1A). For DBC, we find that although DBC concentrations in HMW UDOC quantitively decrease, measured values are not statistically different between the surface (64 ± 23 nM) and deep samples (32 ± 12 nM) (Fig. 1 and *SI Appendix,* Table S1B). LMW SPE-DBC concentrations were also not significantly different between surface and deep waters (670 ± 87 nM and 540 ± 88 nM, respectively). We find that the majority (>90 %) of DBC resides in the LMW SPE-DOC pool in these size-fractionated samples.

The DBC concentrations across size fractions may be controlled by different abiotic and biotic processes (e.g., UV oxidation and microbial degradation) that may preferentially impact DBC
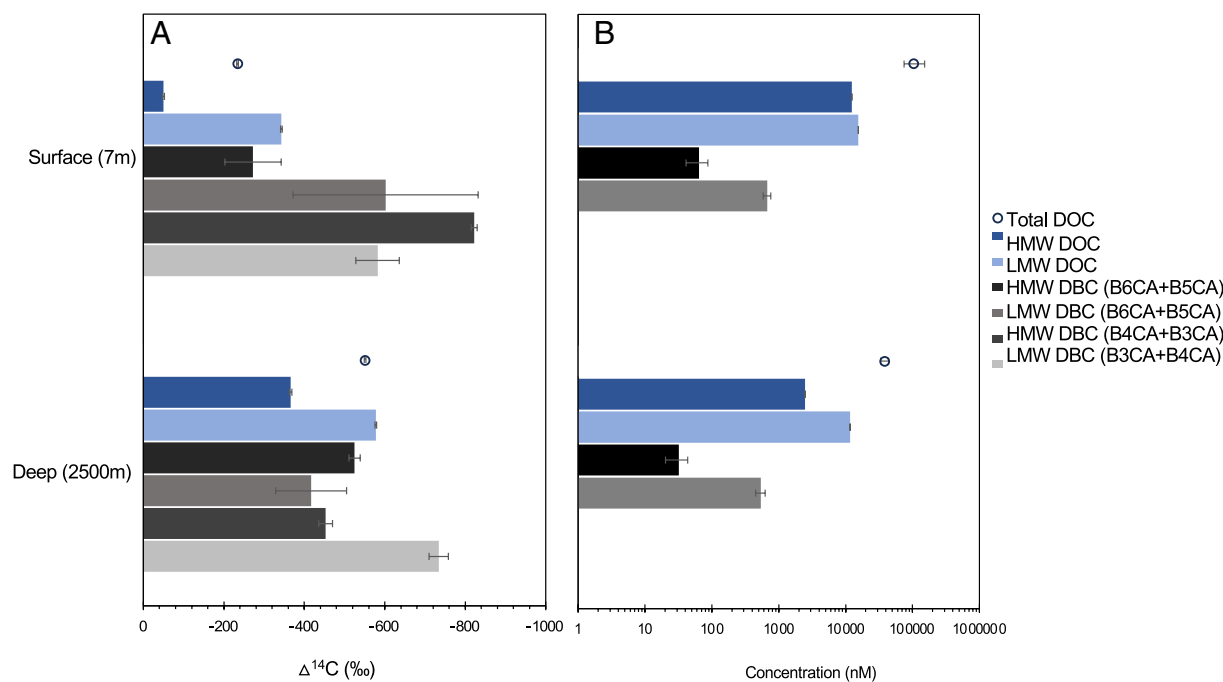
Fig. 1. DOC and DBC (A) Δ^{14}C values and (B) concentrations in surface and deep marine DOC of LMW and HMW size fractions. DBC is present in both HMW and LMW fractions of total DOC, with concentrations of all fractions show on a log scale. LMW and HMW DOC are shown by light and dark blue bars, respectively. Within these size fractions, the DBC Δ^{14}C values are shown in shades of black as more (B6CA+B5CAs) or less polycondensed (B4CA+B3CAs) structures. We show that marine DBC is not one homogenous pool with a uniform ancient age. DOC Δ^{14}C error bars are ±2‰ and listed in *SI Appendix,* Table S1.

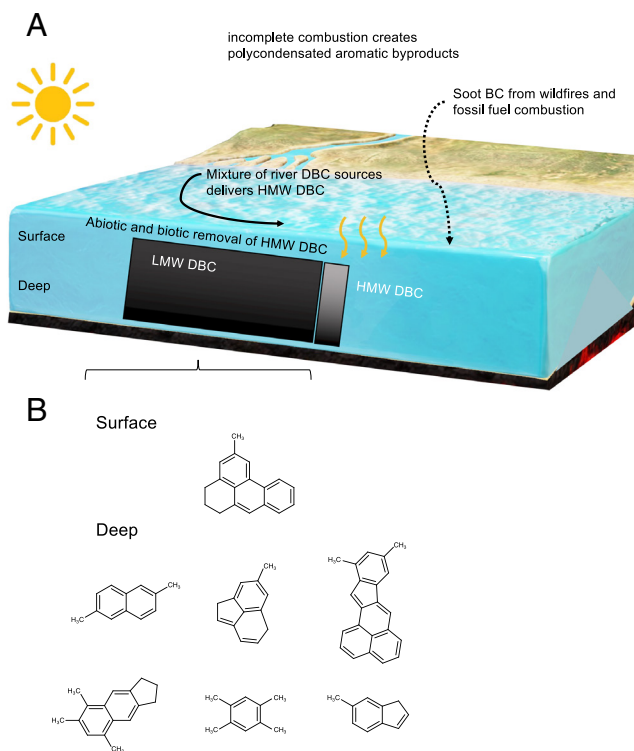**Fig. 2.** (*A*) Overall cycling schematic of DBC in the Central Pacific, showing DBC concentrations based on the relative size of black squares. The production of BC occurs on land through incomplete combustion of biomass and fossil fuels. Rivers transport either recently mobilized DBC from forest fires, DBC that has been stored in intermediate reservoirs on land before transport to the ocean, and fossil fuel derived soot. The majority of DBC is LMW DBC which contributes to the RDOC pool. HMW is lost abiotically (UV oxidation and sorption) or biotically (microbial degradation) in the surface ocean and can contribute to LMW DBC. Fossil fuel–derived DBC from aerosol soot may also be restricted to the surface ocean HMW DBC. (*B*) Measured DBC structures identified using atomic force microscopy in surface and deep LMW DBC from this sample set as in ref. 67.

concentrations in the HMW pool (Fig. 2). Most riverine DBC is associated with the HMW DOC pool (63). One likely mechanism for DBC removal is remineralization by direct UV oxidation (60). HMW DBC is more photolabile than LMW DBC (63), and photodecomposition of HMW DBC generates less polycondensed DBC products that may become associated with the LMW DOC size fractions (63). UV oxidation in turn makes this pool more bioavailable for marine heterotrophs (4, 64). DBC with larger aromatic clusters, or with higher degrees of aromatic condensation is also preferentially lost by UV oxidization (21, 60), potentially explaining the lower concentrations of DBC in HMW DOC than that in LMW SPE-DOC. Given that DBC concentrations in HMW-UDOC are lower than in LMW SPE-DOC, UV oxidization may primarily impact the HMW DBC pool, with lesser impacts on LMW DBC. However, variations in DBC concentrations within HMW and LMW fractions may also be driven by bioavailability, as HMW DBC is more prone to microbial degradation (64). Recent findings from incubation experiments suggest that soot-HMW DBC, biomass-derived BC and photo-oxidized char BC are all bioavailable (4, 64–66), with consumption of soot HMW DBC (64) implying that marine microbes use extracellular enzymes to produce radical oxygen species capable of degrading large molecules into smaller molecules (66).

1.3. DBC Reveals Discrete Cycling with Depth and Aromatic Condensation. Although concentrations of DBC are relatively homogenous with depth for size classes, their respective DBC

structures vary (*SI Appendix*, Table S1*B*). We find heterogeneity in the degree of aromatic condensation among samples. The relationships of DBC structure (expressed as the degree of aromatic condensation from measured BPCA %) are linked to complementary Infrared and ^{13}C solid-state NMR spectroscopy data (55–57, 68). The degree of aromatic condensation in surface HMW-UDOC (65 ± 2% B6CA/sum BPCAs) is higher than that in LMW SPE-DOC (15 ± 2% B6CA/sum BPCAs). In contrast, DBC in HMW SPE-DOC (26 ± 2% B6CA/sum BPCAs) has a lower degree of aromatic condensation than that in LMW SPE-DOC (36 ± 2% B6CA/sum BPCAs) at depth (*SI Appendix*, Table S1*B*). The proportion of more polycondensed (B6CA + B5Cas/total BPCAs %) compared to less polycondensed (B3CA + B4CAs/total BPCAs %) structures shows that this also varies with molecular size and depth, ranging from 62 to 44% (*SI Appendix*, Table S1*B*). Alternatively, differences in diversity could indicate that HMW components of DBC are subjected to a more diverse range of environmental processes (such as aggregation, microbial degradation, and/or photochemical oxidation) than their LMW DBC counterparts. Irrespective of the specific mechanisms influencing the structure of these DBC pools, these differences imply that DBC is composed of a heterogenous pool of components both in terms of molecular size and structure and that this pool is modified dynamically.

1.4. DBC Does Not Comprise a Single, Uniformly Aged Component of RDOC. Although DBC concentrations in HMW UDOC remain similar with depth in the Central Pacific, DBC ^{14}C contents of HMW UDOC decrease, with lowest values at depth for more polycondensed DBC structures, with Δ^{14}C values of –272 ± 70‰ (2,540 ± 780 ^{14}C y) and –525 ± 14‰ (5,970 ± 240 ^{14}C y) in the surface and deep ocean, respectively (Fig. 1). Furthermore, Δ^{14}C values of surface DBC in LMW SPE-DOC are lower than those in HMW UDOC, whereas Δ^{14}C values of LMW SPE-DBC at depth (–602 ± 203‰, 7,400 ± 4,000 ^{14}C y) are similar to those at the surface (–417 ± 88‰, 4,330 ± 1,220 ^{14}C y), given the relatively large measurement uncertainties due to small sample sizes despite processing of relatively large volumes (>2,000 L) of water. Although changes in the degree of aromatic condensation and DBC Δ^{14}C values at depth indicate UV oxidation, biodegradation, sorption, and aggregation processes may be occurring (69), the concentrations of DBC in HMW UDOC are not different between surface and deep due to large error bars. Overall, the DBC Δ^{14}C values imply that dynamic cycling is occurring; concentrations remain stable while DBC Δ^{14}C values differ, which indicates cycling. Examination of the influence of specific processes, such as sorption and photooxidation on Δ^{14}C signatures, is needed in order to elucidate underlying factors and their impact on DBC concentration and isotopic gradients in the ocean.

We also measured Δ^{14}C values of all BPCAs to identify DBC precursor molecules that give rise to the less polycondensed BPCA moieties, which has not yet been measured individually before. We find that the less polycondensed DBC structures (i.e., B3CA and B4CA) are among the most ^{14}C-depleted components of DOC. These products derive from aromatic rings at the periphery of DBC macromolecule(s), whereas B5CA and B6CAs stem from more condensed polyaromatic ring structures. B3CA and B4CAs in HMW UDOC have Δ^{14}C values of –822 ± 7‰ (13,800 ± 300 ^{14}C y) and –453 ± 17‰ (4,800 ± 240 ^{14}C y) in the surface and deep ocean, respectively (*SI Appendix*, Table S1*D*), whereas Δ^{14}C values of corresponding DBC components from LMW SPE-DOC are –582 ± 54‰ (7,000 ± 1,000 ^{14}C y) and –734 ± 24‰ (10,600 ± 720 ^{14}C y) in the surface and deep waters, respectively (*SI Appendix*, Table S1*D*). The lower Δ^{14}C values of the B3CA and B4CAs than bulk DOC and in most depths and in nearly all

size fractions (HMW UDOC and LMW SPE-DOC) suggests that less polycondensed DBC (precursors to these B4CA and B3CAs) may be highly recalcitrant and can survive both photooxidation and biodegradation.

Recent in vitro biodegradation data have shown that soluble fractions of soot DBC, when added to natural seawater, are bioavailable in marine environments (64). The soluble fractions of fossil fuel–derived DBC were added to a marine bacterial incubation experiment and found significant decreases (up to 38%) of DBC over the course of a 3 mo period. Adding different soluble soot DBC treatments to marine environments can significantly modify the chemical environment to which heterotrophic prokaryotes are receptive/sensitive (by causing a shift in bacterial metabolism either favoring anabolism or catabolism) by behaving as a more or less labile source of new DOC and as a source of nutrients and metals. Less condensed DBC molecules were preferentially consumed, which was observed even when measuring polycyclic aromatic hydrocarbon fractions. The coupling of photo-oxidation at the surface with bacterial catabolism revealed the greatest losses of soluble, soot–derived DBC. Here, we find that soot BC, as manifested in B5CA and B6CA (70), in HMW DBC is consumed at depth, implying that it does not contribute a refractory component of DOC, associated with long-term C storage. Thus, LMW DBC is apparently characterized by slower cycling relative to DBC components found in HMW UDOC. In contrast, the uniformly depleted ^{14}C content of LMW DBC suggests that it contributes to the RDOC pool at all depths and cycles similarly throughout the oceans on millennia timescales (71). Given that DBC is the largest and among most persistent components of the LMW DOC pool, it is responsible for most long-term DBC storage in the ocean.

In addition to differences in oceanic turnover, DBC may also exhibit different ^{14}C ages due to different source inputs, ranging from BC from vegetation fires (that may be modern or preaged during intermediate storage on land), or fossil fuel–derived BC. Although atmospheric deposition of fossil fuel–derived DBC to the surface ocean is an order of magnitude smaller (1.8 Tg y^{-1}) (7) than river export of DBC from biomass burning (18 ± 4 Tg y^{-1}) (25), the former in fact may dominate the less condensed DBC in the surface HMW UDOC pool as a consequence of photo-alteration during transit (63, 72).

In the North Central Pacific, we find that HMW UDOC in the surface likely contains soot BC due to the exceptionally low $\Delta^{14}C$ value of the less polycondensed B3CA and B4CAs (–822 ± 7‰, 13,800 ± 300 ^{14}C y; *SI Appendix*, Table S1*D*). The soot from primary fossil fuel burning creates BC rich in B6CAs (62, 70). However, a dominance of B3CA and B4CAs was reported for DBC resulting from the aqueous solution from the dissolution and leaching of soot (73). This may help explain the low $\Delta^{14}C$ value we find in HMW UDOC as depleted in B3CAs and B4CAs (–822 ± 7‰). Atmospheric deposition of water-soluble BC on the surface ocean is highly variable, depending on season, transport pathways, and sources (7). Simple isotopic mass balance calculations suggest that about 16% of soot BC may derive from biomass burning (assuming modern end-member $\Delta^{14}C$ values ranging from 199 to 112‰) (18), given non-fossil-measured $\Delta^{14}C$ values of DBC in ocean waters (i.e., >–1000‰). BC $\Delta^{14}C$ values of background aerosols (in the absence of forest fires) have been as low as –354 ± 60‰ (18, 19), suggesting a mix of fossil fuel–derived soot and biomass aerosols (7, 19, 26). Given that a low $\Delta^{14}C$ signal is not present in HMW DBC at depth, soot-DBC appears to be removed relatively rapidly, presumably as a consequence of biodegradation by marine heterotrophic prokaryotes (16, 64), photochemical degradation and/or sorption and vertical export on sinking particles. In contrast, DBC in LMW SPE-DOC exhibits less-polycondensed characteristics (reflected by the degree of aromatic condensation; *SI Appendix*, Table S1*B*) and is recalcitrant. Sources of hydrothermal DBC could be investigated as additional inputs.

2. Implications and Future Work

We find that DBC is a large fraction of RDOC, the largest fraction that has been measured by combining two DOC collection methods. Since $\Delta^{14}C$ measurements of individual BPCAs in size-fractionated DOC samples require processing of very large volumes of water (1,000s of L), the number of samples reported here is necessarily limited. However, to date, no other studies have captured half of marine DBC. Ultimately, while SPE retentate may not represent all RDOC, its very old ^{14}C ages indicate that it is a good proxy for the most long-lived RDOC in the ocean. We note that our $\Delta^{14}C$ value of central Pacific DBC in the ocean (surface DBC value in HMW UDOM –822 ± 7‰, *SI Appendix*, Table S1*D*) is similar to a previous measurement of DBC in HMW UDOM in the central Pacific (–880 ± 38‰) (10). Determining how DBC is distributed across these size and chemical fractions is of importance when comparing river and marine samples given the contrasting techniques that are usually applied to freshwater and marine matrices.

Possible exchange between the dissolved and PBC pools, in particular HMW pools, is a mechanism that may also be important (30) in the data we report. Particles and particle remineralization at depth may act as a source of DBC to the subsurface (69), while aggregation of DBC in HMW UDOC and export onto sinking particles (74) may lead to removal from the surface ocean and transfer to underlying sediments (75). We speculate that this latter mechanism may be important for transporting fossil fuel–derived DBC in HMW UDOC to POC and subsequently to sediments (74), while smaller, hydrophilic DBC structures (reflected by B3CAs-B4CAs) preferentially accumulate in oceanic DOC as previous work found that the oldest BPCAs had DBC with lower degrees of aromatic condensation (10, 76, 77). This idea is supported by a sorption-enhanced phototransformation documented with hydrophobic organic contaminants (75).

3. Conclusions

Our results indicate that DBC is distributed unevenly across DOC size classes and does not comprise a single, uniformly aged refractory component of RDOC. Instead, DBC consists of a range of constituents that differ in molecular size and degree of aromatic condensation. While DBC concentrations are relatively invariant with depth, differences in DBC $\Delta^{14}C$ values in the surface and deep waters suggest the existence of separate DBC pools (HMW separate from LMW) or different DBC sources (soot, biomass) that are more susceptible to specific removal mechanisms. Overall, our results suggest that the less aromatic DBC structures in marine DOC may have undergone chemical modification (for example, photo-oxidation) and derive from soot in HMW size fractions (B3CA and B4CA as the soluble soot by-products) (70), thereby increasing their bioavailability for bacterial remineralization (64). The $\Delta^{14}C$ values of DBC in size-fractionated HMW UDOC and LMW SPE-DOC, as well as specific BPCA markers, provide evidence for variable cycling and storage of different pools of DBC in the ocean. The variability of the DBC structures (given by the degree of aromatic condensation) and ages ($\Delta^{14}C$ values) among molecular size classes in surface and deep ocean DOC samples implies that DBC may reflect different inputs and experience diverse environmental fates and cycling dynamics.

4. Methods

The collection of North Central Pacific seawater samples and DOC size fractions has been described previously (41, 53) (*SI Appendix*, section 1.1). Briefly, seawater was collected using Niskin bottles in the surface (7 m) and deep (2,500 m) locations of the HOT Series Station ALOHA (22°25′N, 158°00′W). Seawater was filtered through a 0.2 μm cartridge filter to remove particulate organic matter and then ultrafiltered (UF) with 2.5 kD tangential flow ultrafiltration membranes to isolate HMW UDOC and dried. The permeate of the UF system (<2.5 kD) was acidified to pH 2 and concentrated by sorption onto a SPE resin. The sorbed, LMW SPE-DOM was then desalted with Milli-Q water, eluted with methanol, and dried.

DBC was extracted from HMW UDOC and LMW SPE-DOM samples using the BPCA chemical oxidation method that oxidizes condensed aromatic structures to produce a mixture of benzenetricarboxylic acids (B3CA: 1,2,3-B3CA and 1,2,4- B3CA), benzenetetracarboxylic acid (B4CAs: 1,2,4,5-B4CA), benzenepentacarboxylic acid (B5CA), and benzenehexacarboxylic acids (B6CA) (78). DBC concentrations were calculated by applying a conversion to BPCA yields (79), while the relative abundance of BPCA markers was used to determine DBC polycondensed structure. The relative abundance of BPCA marker compounds produced via laboratory chemical oxidation provides estimates of the degree of aromatic condensation (56, 57). BPCA ratios ([B6]/[sum of all BPCAs]) indicate the degree of aromatic condensation of the DBC pool based on complimentary method comparisons with ^{13}C solid state-NMR studies (56, 57). Specifically, higher ratios indicate an overall high aromatic condensation network. Finally, we applied compound-specific radiocarbon ($\Delta^{14}C$) analysis of BPCAs to determine DBC $\Delta^{14}C$ values for the same samples.

1. A. I. Coppola *et al.*, The black carbon cycle and its role in the Earth system. *Nat. Rev. Earth Environ.* **3**, 516–532 (2022).
2. E. D. Goldberg, *Black Carbon in the Environment: Properties and Distribution* (John Wiley and Sons, New York, NY, 1985), pp. Medium: X; Size: Pages: 198 2008-2002-2006.
3. T. W. Drake *et al.*, Du Feu à l'Eau: Source and flux of dissolved black carbon from the Congo River. *Global Biogeochem. Cycles* **34**, e2020GB006560 (2020).
4. K. W. Bostick *et al.*, Biolability of fresh and photodegraded pyrogenic dissolved organic matter from laboratory-prepared chars. *J. Geophys. Res. Biogeosci.* **126**, e2020JG005981 (2021).
5. M. W. Jones, C. Santín, G. R. van der Werf, S. H. Doerr, Global fire emissions buffered by the production of pyrogenic carbon. *Nat. Geosci.* **12**, 742–747 (2019).
6. X. Wei, D. J. Hayes, S. Fraver, G. Chen, Global pyrogenic carbon production during recent decades has created the potential for a large, long-term sink of atmospheric CO2. *J. Geophys. Res. Biogeosci.* **123**, 3682–3696 (2018).
7. H. Bao, J. Niggemann, L. Luo, T. Dittmar, S. Kao, Aerosols as a source of dissolved black carbon to the ocean. *Nat. Commun.* **8**, 510 (2017).
8. T. C. Bond *et al.*, Bounding the role of black carbon in the climate system: A scientific assessment. *J. Geophys. Res. Atmos.* **118**, 5380–5552 (2013).
9. A. I. Coppola, E. R. M. Druffel, Cycling of black carbon in the ocean. *Geophys. Res. Lett.* **43**, 4477 (2016).
10. L. A. Ziolkowski, E. R. M. Druffel, Aged black carbon identified in marine dissolved organic carbon. *Geophys. Res. Lett.* **37**, L16601 (2010).
11. D. M. J. S. Bowman *et al.*, Vegetation fires in the Anthropocene. *Nat. Rev. Earth Environ.* **1**, 500–515 (2020).
12. M. W. Jones *et al.*, Global and regional trends and drivers of fire under climate change. *Rev. Geophys.* **60**, e2020RG000726 (2022).
13. J.-S. Landry, H. D. Matthews, The global pyrogenic carbon cycle and its impact on the level of atmospheric CO2 over past and future centuries. *Global Change Biol.* **23**, 3205–3218 (2017).
14. S. P. K. Bowring, M. W. Jones, P. Ciais, B. Guenet, S. Abiven, Pyrogenic carbon decomposition critical to resolving fire's role in the Earth system. *Nat. Geosci.* **15**, 135–142 (2022).
15. C. Santin, S. H. Doerr, C. M. Preston, G. Gonzalez-Rodriguez, Pyrogenic organic matter production from wildfires: A missing sink in the global carbon cycle. *Global Change Biol.* **21**, 1621–1633 (2015).
16. Y. Qi *et al.*, Dissolved black carbon is not likely a significant refractory organic carbon pool in rivers and oceans. *Nat. Commun.* **11**, 5051 (2020).
17. C. Santín *et al.*, Towards a global assessment of pyrogenic carbon from vegetation fires. *Global Change Biol.* **22**, 76–91 (2016).
18. G. O. Mouteva *et al.*, Black carbon aerosol dynamics and isotopic composition in Alaska linked with boreal fire emissions and depth of burn in organic soils. *Global Biogeochem. Cycles* **29**, 1977–2000 (2015).
19. G. O. Mouteva *et al.*, Using radiocarbon to constrain black and organic carbon aerosol sources in Salt Lake City. *J. Geophys. Res. Atmos.* **122**, 9843–9857 (2017).
20. M. Reisser, R. S. Purves, M. W. I. Schmidt, S. Abiven, Pyrogenic carbon in soils: A literature-based inventory and a global estimation of its content in soil organic carbon and stocks. *Front. Earth Sci.* **4**, 80 (2016).
21. K. W. Bostick *et al.*, Photolability of pyrogenic dissolved organic matter from a thermal series of laboratory-prepared chars. *Sci. Total Environ.* **724**, 138198 (2020).
22. N. Trilla-Prieto, M. Vila-Costa, G. Casas, B. Jiménez, J. Dachs, Dissolved black carbon and semivolatile aromatic hydrocarbons in the ocean: Two entangled biogeochemical cycles? *Environ. Sci. Technol. Lett.* **8**, 918–923 (2021).
23. C. A. Masiello, A. A. Berhe, First interactions with the hydrologic cycle determine pyrogenic carbon's fate in the Earth system. *Earth Surf. Processes Landforms* **45**, 2394–2398 (2020).
24. A. I. Coppola *et al.*, Global-scale evidence for the refractory nature of riverine black carbon. *Nat. Geosci.* **11**, 584–588 (2018).
25. M. W. Jones *et al.*, Fires prime terrestrial organic carbon for riverine export to the global oceans. *Nat. Commun.* **11**, 2791 (2020).
26. X. Wang, C. Xu, E. R. M. Druffel, Y. Xue, Y. Qi, Two black carbon pools transported by the Changjiang and Huanghe Rivers in China. *Global Biogeochem. Cycles* **30**, 1778 (2016).
27. T. Dittmar *et al.*, Continuous flux of dissolved black carbon from a vanished tropical forest biome. *Nat. Geosci.* **5**, 618–622 (2012).
28. R. Barton *et al.*, Hydrology, rather than wildfire burn extent, determines post-fire organic and black carbon export from mountain rivers in central coastal California. *Limnol. Oceanogr. Lett.* **9**, 70–80 (2024).
29. R. B. Abney *et al.*, Pyrogenic carbon erosion after the Rim Fire, Yosemite National Park: The role of burn severity and slope. *J. Geophys. Res. Biogeosci.* **124**, 432–449 (2019).
30. Y. Fang *et al.*, Particulate and dissolved black carbon in coastal China seas: Spatiotemporal variations, dynamics, and potential implications. *Environ. Sci. Technol.* **55**, 788–796 (2021).
31. S. Wagner *et al.*, Isotopic composition of oceanic dissolved black carbon reveals non-riverine source. *Nat. Commun.* **10**, 5064 (2019).
32. S. Wagner, R. Jaffé, A. Stubbins, Dissolved black carbon in aquatic ecosystems. *Limnol. Oceanogr. Lett.* **3**, 168–185 (2018).
33. D. A. Hansell, C. A. Carlson, D. J. Repeta, R. Schlitzer, Dissolved organic matter in the ocean a controversy stimulates new insights. *Oceanography* **22**, 202–211 (2009).
34. T. S. Catalá, S. Shorte, T. Dittmar, Marine dissolved organic matter: A vast and unexplored molecular space. *Appl. Microbiol. Biotechnol.* **105**, 7225–7239 (2021).
35. B. D. Walker, S. R. Beaupré, T. P. Guilderson, M. D. McCarthy, E. R. M. Druffel, Pacific carbon cycling constrained by organic matter size, age and composition relationships. *Nat. Geosci.* **9**, 888–891 (2016).
36. E. R. M. Druffel, Bomb radiocarbon in the Pacific–Annual and seasonal timescale variations. *J. Marine Res.* **45**, 667–698 (1987).
37. E. R. M. Druffel, S. Griffin, Radiocarbon in dissolved organic carbon of the South Pacific Ocean. *Geophys. Res. Lett.* **42**, 4096–4101 (2015).
38. D. A. Hansell, Recalcitrant dissolved organic carbon fractions. *Annu. Rev. Marine Sci.* **5**, 421–445 (2013).
39. R. Benner, R. M. W. Amon, The size-reactivity continuum of major bioelements in the ocean. *Annu. Rev. Marine Sci.* 7, 185–205 (2015).
40. B. D. Walker, S. R. Beaupré, T. P. Guilderson, M. D. McCarthy, E. R. M. Druffel, Pacific carbon cycling constrained by organic matter size, age and composition relationships. *Nat. Geosci.* **9**, 888 (2016).
41. T. A. B. Broek, B. D. Walker, T. P. Guilderson, M. D. McCarthy, Coupled ultrafiltration and solid phase extraction approach for the targeted study of semi-labile high molecular weight and refractory low molecular weight dissolved organic matter. *Marine Chem.* **194**, 146–157 (2017).
42. T. Dittmar, J. Paeng, A heat-induced molecular signature in marine dissolved organic matter. *Nat. Geosci.* **2**, 175–179 (2009).
43. A. I. Coppola, E. R. M. Druffel, Cycling of black carbon in the ocean. *Geophys. Res. Lett.* **43**, 4477–4482 (2016).
44. R. Cai, N. Jiao, Recalcitrant dissolved organic matter and its major production and removal processes in the ocean. *Deep Sea Res. Part I: Oceanogr. Res. Papers* **191**, 103922 (2023).
45. T. Dittmar *et al.*, Enigmatic persistence of dissolved organic matter in the ocean. *Nat. Rev. Earth Environ.* **2**, 570–583 (2021).
46. N. Jiao *et al.*, Microbial production of recalcitrant dissolved organic matter: Long-term carbon storage in the global ocean. *Nat. Rev. Microbiol.* **8**, 593–599 (2010).
47. A. Mentges, C. Feenders, C. Deutsch, B. Blasius, T. Dittmar, Long-term stability of marine dissolved organic carbon emerges from a neutral network of compounds and microbes. *Sci. Rep.* **9**, 17780 (2019).
48. J. M. Arrieta *et al.*, Dilution limits dissolved organic carbon utilization in the deep ocean. *Science* **348**, 331–333 (2015).
49. Y. Yamashita, Y. Mori, H. Ogawa, Hydrothermal-derived black carbon as a source of recalcitrant dissolved organic carbon in the ocean. *Sci. Adv.* **9**, eade3807 (2023).
50. J. Brünjes, M. Seidel, T. Dittmar, J. Niggemann, F. Schubotz, Natural asphalt seeps are potential sources for recalcitrant oceanic dissolved organic sulfur and dissolved black carbon. *Environ. Sci. Technol.* **56**, 9092–9102 (2022), 10.1021/acs.est.2c01123.
51. M. D. McCarthy *et al.*, Chemosynthetic origin of 14C-depleted dissolved organic matter in a ridge-flank hydrothermal system. *Nat. Geosci.* **4**, 32–36 (2011).
52. J. W. Pohlman, J. E. Bauer, W. F. Waite, C. L. Osburn, N. R. Chapman, Methane hydrate-bearing seeps as a source of aged dissolved organic carbon to the oceans. *Nat. Geosci.* **4**, 37–41 (2011).
53. T. A. B. Broek *et al.*, Low molecular weight dissolved organic carbon: Aging, compositional changes, and selective utilization during global ocean circulation. *Global Biogeochem. Cycles* **34**, e2020GB006547 (2020).
54. T. Dittmar, The molecular level determination of black carbon in marine dissolved organic matter. *Org. Geochem.* **39**, 396–407 (2008).
55. A. V. McBeath, R. J. Smernik, M. P. W. Schneider, M. W. I. Schmidt, E. L. Plant, Determination of the aromaticity and the degree of aromatic condensation of a thermosequence of wood charcoal using NMR. *Org. Geochem.* **42**, 1194–1202 (2011).
56. D. B. Wiedemeier *et al.*, Aromaticity and degree of aromatic condensation of char. *Org. Geochem.* **78**, 135–143 (2015).

57. A. Budai et al., Effects of pyrolysis conditions on Miscanthus and corncob chars: Characterization by IR, solid state NMR and BPCA analysis. *J. Anal. Appl. Pyrolysis* **128**, 335–345 (2017).

58. Y. Kuzyakov, I. Bogomolova, B. Glaser, Biochar stability in soil: Decomposition during eight years and transformation as assessed by compound-specific C-14 analysis. *Soil Biol. Biochem.* **70**, 229–236 (2014).

59. Y. Fang, B. Singh, B. P. Singh, E. Krull, Biochar carbon stability in four contrasting soils. *Eur. J. Soil Sci.* **65**, 60–71 (2014).

60. A. Stubbins, J. Niggemann, T. Dittmar, Photo-lability of deep ocean dissolved black carbon. *Biogeosciences* **9**, 1661–1670 (2012).

61. B. Glaser, L. Haumaier, G. Guggenberger, W. Zech, Black carbon in soils: The use of benzenecarboxylic acids as specific markers. *Org. Geochem.* **29**, 811–819 (1998).

62. L. A. Ziolkowski, A. R. Chamberlin, J. Greaves, E. R. M. Druffel, Quantification of black carbon in marine systems using the benzene polycarboxylic acid method: A mechanistic and yield study. *Limnol. Oceanogr. Methods* **9**, 140–149 (2011).

63. S. Wagner, R. Jaffe, Effect of photodegradation on molecular size distribution and quality of dissolved black carbon. *Org. Geochem.* **86**, 1–4 (2015).

64. P. L. Martinot et al., Assessing the bioavailability of black carbon-derived dissolved organic matter for marine heterotrophic prokaryotes. *Sci. Total Environ.* **901**, 165802 (2023), 10.1016/j.scitotenv.2023.165802.

65. A. I. Goranov et al., Photochemistry after fire: Structural transformations of pyrogenic dissolved organic matter elucidated by advanced analytical techniques. *Geochim. Cosmochim. Acta* **290**, 271–292 (2020).

66. A. I. Goranov et al., Microbial labilization and diversification of pyrogenic dissolved organic matter. *Biogeosciences* **19**, 1491–1514 (2022).

67. S. Fatayer et al., Direct visualization of individual aromatic compound structures in low molecular weight marine dissolved organic carbon. *Geophys. Res. Lett.* **45**, 5590–5598 (2018).

68. A. V. McBeath, R. J. Smernik, Variation in the degree of aromatic condensation of chars. *Org. Geochem.* **40**, 1161–1168 (2009).

69. Y. Yamashita, M. Nakane, Y. Mori, J. Nishioka, H. Ogawa, Fate of dissolved black carbon in the deep Pacific Ocean. *Nat. Commun.* **13**, 307 (2022).

70. P. J. Roth et al., Differentiation of charcoal, soot and diagenetic carbon in soil: Method comparison and perspectives. *Org. Geochem.* **46**, 66–75 (2012).

71. C. A. Masiello, E. R. M. Druffel, Black carbon in deep-sea sediments. *Science* **280**, 1911–1913 (1998).

72. A. L. Khan, R. Jaffe, Y. Ding, D. M. McKnight, Dissolved black carbon in Antarctic lakes: Chemical signatures of past and present sources. *Geophys. Res. Lett.* **43**, 5750–5757 (2016).

73. Y. Ding, Y. Yamashita, J. Jones, R. Jaffe, Dissolved black carbon in boreal forest and glacial rivers of central Alaska: Assessment of biomass burning versus anthropogenic sources. *Biogeochemistry* **123**, 15–25 (2015).

74. A. I. Coppola, L. A. Ziolkowski, C. A. Masiello, E. R. M. Druffel, Aged black carbon in marine sediments and sinking particles. *Geophys. Res. Lett.* **41**, 2427–2433 (2014).

75. H. Wang, M. Han, M. Wang, H. Zhou, Microheterogeneous triplet oxidation of hydrophobic organic contaminants in dissolved black carbon solutions under simulated solar irradiation. *Environ. Sci. Technol.* **56**, 14574–14584 (2022).

76. S. Wagner, R. Jaffé, A. Stubbins, Dissolved black carbon in aquatic ecosystems. *Limnol. Oceanogr. Lett.* **3**, 168 (2018).

77. C. Masiello, P. Louchouarn, Fire in the Ocean. *Science* **340**, 287 (2013).

78. T. Dittmar, The molecular level determination of black carbon in marine dissolved organic matter. *Org. Geochem.* **39**, 396 (2008).

79. L. A. Ziolkowski, A. R. Chamberlin, J. Greaves, E. R. M. Druffel, Quantification of black carbon in marine systems using the benzene polycarboxylic acid method: A mechanistic and yield study. *Limnol. Oceanogr.: Methods* **9**, 140 (2011).